

Generalizable deep learning forecasting of harmful algal blooms using transfer learning across river systems

Jaegwan Park^a, Taeseung Park^a, Dogeon Lee^a, Jihoon Shin^a, Kyunghyun Kim^b,
Jonggyu Jung^a, Hongtae Kim^{b,*}, YoonKyung Cha^{a,*}

^a School of Environmental Engineering, University of Seoul, Dongdaemun-gu, Seoul 02504, Republic of Korea

^b Han River Environmental Research Center, Water Environment Research Department, National Institute of Environmental Research, Republic of Korea

ARTICLE INFO

Keywords:

Transfer learning
Transformer
Deep learning
Harmful algal blooms
Cyanobacteria, data scarcity

ABSTRACT

Harmful algal blooms (HABs) present serious challenges to water quality and resource management, with their frequency and severity escalating due to climate change and anthropogenic impacts. While deep learning (DL) models show strong predictive capabilities in HAB forecasting, challenges remain due to data scarcity and site-specific variability. This study systematically investigates transfer learning (TL) to improve the generalization and accuracy of HAB forecasts across 26 monitoring sites spanning four major rivers in South Korea. The analysis considers multiple dimensions influencing TL performance, including DL architectures, TL schemes, river system differences, and target domain sample sizes. Various DL architectures were evaluated: the Temporal Fusion Transformer (TFT), Transformer, CNN-LSTM with attention, and recurrent neural network (RNN)-based models. While RNN-based models have been commonly used in TL-based HAB forecasting, advanced architectures like TFT remain unexplored. To evaluate their effectiveness, four TL schemes with varying parameter adaptation were applied, consistently improving forecasting performance across all models and sites. Average R^2 increasing from 0.35 to 0.50 to 0.47–0.60, while site-specific values reaching 0.89. Improvements ranged from 12.51 % to 82.49 %, demonstrating robust generalization gains. Among TL schemes, full fine-tuning yielded the highest number of best-performing sites, especially for transformer-based models. The TFT achieved the strongest overall performance, outperforming others on most sites. Sites with higher cyanobacterial abundance generally exhibited stronger performance, while low-performing sites experienced substantial improvement. Furthermore, SHAP analysis identified key environmental drivers to enhance interpretability and management relevance. This study provides a scalable, transferable framework for advancing DL-based HAB forecasting in data-scarce environments, offering insights for early warning systems and broader environmental applications.

1. Introduction

Harmful algal blooms (HABs), particularly those caused by cyanobacteria, pose substantial risks to aquatic ecosystems, drinking water supplies, and public health due to their ability to produce cyanotoxins and generate unpleasant odors (Carmichael, 2001; Dodds et al., 2009; Paerl and Otten, 2013). The increasing frequency, intensity, and geographic spread of HABs have been attributed to climate change and anthropogenic activities, including rising global temperatures and excessive nutrient loading from agricultural runoff and wastewater discharge (Carey et al., 2012; Dai et al., 2023; Paerl and Huisman, 2008; Wells et al., 2015). As these stressors continue to intensify, HAB

occurrences are becoming more difficult to predict and manage, necessitating accurate and timely forecasting. Reliable forecasting models play a critical role in supporting early warning systems, guiding proactive water resource management strategies, and enabling timely mitigation efforts to minimize ecological and economic losses (Burford et al., 2020; Davidson et al., 2016).

Advancements in big data and computational power have facilitated the widespread adoption of data-driven artificial intelligence (AI) models for water quality prediction, including HAB forecasting (Cruz et al., 2021; Rousoo et al., 2020). Among various AI-based approaches for HAB forecasting, deep learning (DL) models have demonstrated superior predictive performance due to their ability to capture complex

* Corresponding authors.

E-mail addresses: jp0926@uos.ac.kr (J. Park), alex1001@uos.ac.kr (T. Park), ehrjs2000@uos.ac.kr (D. Lee), khkim@korea.kr (K. Kim), whdrb1049@uos.ac.kr (J. Jung), htkim8@korea.kr (H. Kim), ykcha@uos.ac.kr (Y. Cha).

relationships within large datasets (Goodfellow et al., 2016; Schmidhuber, 2015). Previous studies have widely applied Recurrent Neural Network (RNN)-based models for HAB forecasting due to their ability to capture sequential dependencies in time-series data (Cruz et al., 2021; Hill et al., 2020; Lee and Lee, 2018). In particular, Long Short-Term Memory (LSTM) networks have demonstrated robust performance by effectively capturing long-term temporal dependencies and nonlinear relationships among environmental factors. LSTM models have been extensively used to predict temporal patterns of water quality parameters, including chlorophyll-a concentrations, and to analyze meteorological influences in HAB forecasting (Busari et al., 2025; Fournier et al., 2024; Lin et al., 2023; Shin et al., 2020; Yussof et al., 2021). Beyond RNN-based models, more advanced approaches have employed Graph Neural Networks (GNNs) and hybrid deep learning frameworks to explicitly capture spatial dependencies across monitoring sites, achieving improved forecasting accuracy in multi-site or river network systems (Kim et al., 2024; Jia et al., 2024; Meng et al., 2025; Shin and Cha, 2025). More recently, developments in DL have introduced Transformer-based architecture, which has demonstrated outstanding performance in HAB forecasting by effectively capturing long-range dependencies and processing heterogeneous temporal data (Ahn et al., 2023; Chen et al., 2025; Li et al., 2025). In contrast to traditional RNN-based models that rely on sequential processing, Transformer models employ a self-attention mechanism, enabling them to capture global dependencies across time-series data efficiently (Vaswani et al., 2017). The multi-head self-attention mechanism enhances this capability by attending to multiple temporal patterns, improving the modeling of complex environmental interactions. Positional encoding compensates for the lack of inherent sequential structure, ensuring effective time-series modeling. Building upon these advancements, the Temporal Fusion Transformer (TFT) enhances multivariate time-series forecasting by incorporating gated mechanisms and attention-based components, resulting in improved predictive performance across complex temporal patterns (Lim et al., 2019).

While the DL models have substantially improved HAB forecasting, they still face significant challenges. These models require large volumes of labeled training data for robust and generalizable performance (Zhu and Wu, 2004). However, such data is often scarce in HAB monitoring (Janssen et al., 2019; Wells et al., 2015). Furthermore, the high costs of in situ measurements and the complex interactions among multiple influencing factors, such as water quality parameters, hydrological conditions, and meteorological variables, further hinder the development of accurate forecasting models (Coad et al., 2014; Marcé et al., 2016). For instance, Demiray et al. (2025) emphasized that LSTMs need substantial labeled data to effectively learn long-term dependencies, posing significant challenges due to the high costs and logistical difficulties of extensive in situ collection for HAB forecasting.

To address these limitations, this study investigates the application of transfer learning (TL) in HAB forecasting. TL facilitates the adaptation of a pre-trained model from a data-rich source to a target domain with limited labeled data, enhancing predictive accuracy while reducing reliance on extensive site-specific training datasets (Weiss et al., 2016; Zhuang et al., 2021). Therefore, integrating TL into the modeling framework is expected to improve HAB forecasting accuracy, especially in data-scarce sites. TL has been widely explored in environmental modeling to address data limitations and improve predictive performance (Ma et al., 2024; Subel et al., 2023). Studies have shown its effectiveness in water quality prediction by leveraging knowledge from data-rich regions to improve models in data-scarce areas. For example, Zhu et al. (2021) applied TL to predict dissolved oxygen (DO) concentrations by pre-training a model on one lake and adapting it to another lake with limited data. Similarly, Chen et al. (2024a) demonstrated cross-location TL, adapting models trained on one river system to various monitoring sites, while Chen et al. (2024b) explored multi-scheme TL with different fine-tuning strategies to assess generalization. Recently, TL has been integrated into Transformer-based

architectures for water quality forecasting. Wang et al. (2024) proposed a Many-to-Many Domain Adaptation (M2M) framework using transformers with domain adaptation to enhance generalization across monitoring sites. Peng et al. (2022) introduced the TL based on Transformer (TLT) model, incorporating fine-tuning strategies to improve long-term water quality predictions. For HAB forecasting, however, while TL has been combined with DL models such as LSTMs (Ni et al., 2022), its integration with Transformer-based architecture remains underdeveloped.

This study systematically applies TL across various DL architectures to address data scarcity and enhance model generalization in HAB forecasting. By integrating TL across multiple architectures and geographic locations, this approach aims to improve model adaptability and scalability, making it more applicable for real-world forecasting. Specifically, this study aims to: (1) compare the performance of different DL models, including Transformer-based models, when integrated with TL, (2) assess the impact of site-specific HAB intensity on TL effectiveness, (3) evaluate the forecasting accuracy and generalization ability of various TL schemes (4) examine the influence of sample size at the target site on TL effectiveness and (5) identify key drivers of HAB forecasts using the TL-based model. The insights gained from this study are expected to enhance the effectiveness of HABs early warning systems and improve the reliability of data-driven water quality management. Additionally, the findings provide valuable guidance for other data-scarce domains that could benefit from integrating TL with DL approaches.

2. Material and methods

2.1. Study area and data description

The study area encompassed the four major rivers of South Korea—the Han, Geum, Yeongsan, and Nakdong River—which have experienced an increasing occurrence of HABs in recent years. The four rivers differ in length and watershed area: the Han River is 494 km long with a watershed area of 25,953 km², the Geum River is 398 km long with 9912 km², the Yeongsan River is 130 km long with 3467 km², and the Nakdong River, the longest, extends 510 km, with a watershed area of 23,384 km². Across these rivers, 16 weirs are distributed, with three each in the Han and Geum Rivers, two in the Yeongsan River, and eight in the Nakdong River. Cyanobacteria monitoring sites are primarily located upstream of these weirs, with additional sites in selected regions. To enhance the generalization of TL, the largest possible dataset from nationwide monitoring sites was utilized. Out of 44 available sites, four with low bloom frequency in the mainstream Han River, four newly established in 2024, and ten monitored only in the summers of 2022 and 2023 were excluded. Ultimately, TL was applied to 26 selected monitoring sites, comprising twelve in the Nakdong River, nine in the Han River, three in the Geum River, and two in the Yeongsan River (Fig. 1).

The data for this study were collected from various monitoring sites between 2012 and 2023, though availability varied by site. Biological and water quality data were obtained from the National institute of environmental research (NIER), Ministry of Environment (<https://water.nier.go.kr>). Hydrological data were obtained from K-water (<https://water.or.kr>) and Han River Flood Control Office (<https://www.hrfco.go.kr>). Meteorological data were sourced from Automated Surface Observing System by Korea Meteorological Administration (<https://kma.go.kr>).

Cyanobacteria cell counts, the primary indicator of HABs, represent the total abundance of four major harmful cyanobacteria genus: *Microcystis*, *Aphanizomenon*, *Dolichospermum* (*Anabaena*), and *Oscillatoria* (NIER, 2023). While cyanobacteria cell counts are typically recorded weekly, if the cell counts exceed the Warning Level ($\geq 10,000$ cells/mL) twice consecutively, as defined by Harmful Algal Bloom Alert System of South Korea, the monitoring frequency increases to semiweekly until the counts drop below the Attention Level (< 1000 cells/mL).

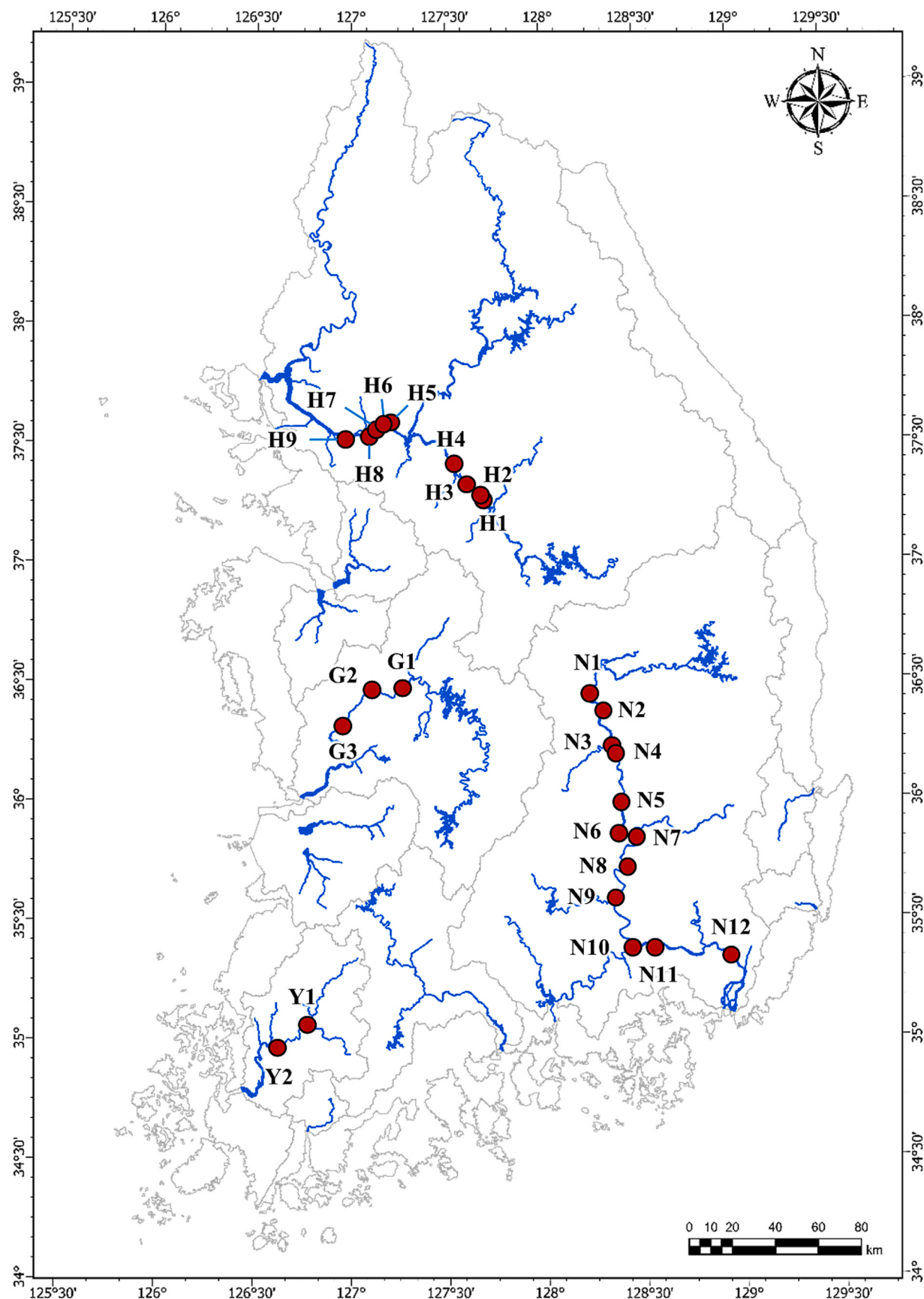


Fig. 1. Map of the study sites in South Korea. The initial of each site is labeled as H for Han River, G for Geum River, Y for Yeongsan River, and N for Nakdong River.

Environmental, hydrological, and meteorological data related to cyanobacterial cell counts were selected as input features, with each monitoring site matched to the nearest available data source (Table 1). Chlorophyll-a (Chl-a) and water temperature (WT) are measured alongside cyanobacteria cell counts weekly to semi-weekly. Other water quality variables, including total nitrogen (TN) and total phosphorus (TP), had varying monitoring frequencies depending on the site. At sites with designated water quality monitoring stations, TN and TP are measured weekly. In contrast, at sites without designated water quality stations relied on data from the nearest available station, typically resulting in less frequent (weekly to monthly) measurements and leading to sparser data availability. Hydrological and meteorological variables, which are monitored daily at locations nearest to cyanobacteria monitoring sites. Hydrological data included total discharge and water level at each monitoring site, as well as upstream total discharge and water level from nearby hydraulic structures (dams or weirs) when applicable. Meteorological data comprised air temperature, precipitation, and forecast temperature. For consistency, water level, air temperature, and forecast temperature were averaged over the seven days preceding each cyanobacteria measurement, while total discharge and precipitation were summed over the same period to reflect cumulative effects.

2.2. Model development

This study aims to generalize the applicability of TL in forecasting HABs by applying various TL schemes (Section 2.2.1) to cyanobacteria monitoring sites in South Korea. A variety of DL models were employed to achieve this objective, including RNN-based models such as Long Short-Term Memory (LSTM), Bidirectional LSTM (Bi-LSTM), and Gated Recurrent Unit (GRU), as well as advanced architectures, including CNN-LSTM with attention (CLA) mechanisms, the Transformer model, and the Temporal Fusion Transformer (TFT) (Section 2.2.2). The model development process (Fig. 2) involved comprehensive data acquisition, data preprocessing, model training, validation, testing (Section 2.2.2), and performance evaluation (Section 2.2.3), ensuring robustness and reliability while evaluating the effectiveness of TL schemes in different

site conditions.

2.2.1. TL schemes

TL facilitates knowledge transfer from data-rich environments (source domain) to data-scarce environments (target domain), enhancing model generalizability in settings with limited training data. TL can be broadly categorized based on the type of knowledge being transferred: instance-based, feature-based, parameter-based, and relational-based approaches (Weiss et al., 2016; Zhuang et al., 2021). Among these, parameter-based TL, which transfers model parameters learned from the source domain to the target domain, is the most widely used in DL applications (Ma et al., 2024). This approach leverages pre-trained weights as initialization, which helps accelerate and stabilize convergence during training, leading to more reliable model optimization (He et al., 2019; Mosbach et al., 2020). A common form of parameter-based TL is fine-tuning, where a pre-trained model is adapted to a new task by updating its parameters with a smaller dataset from the target domain. Fine-tuning can be implemented in multiple ways depending on the degree of adaptation required. Full fine-tuning updates all layers of the model, allowing it to fully adapt to the new domain, whereas model-freezing preserves the pre-trained layers while fine-tuning only a subset of layers responsible for task-specific representations (Feng et al., 2024).

To improve the generalization of applying TL in HAB forecasting, this study employs four TL schemes (Fig. 3) to assess different adaptation strategies. The first scheme (S1), full fine-tuning, updates all model parameters using the target dataset, ensuring complete adaptation while leveraging knowledge from the source domain to learn site-specific patterns (Dosovitskiy et al., 2020; Kornblith et al., 2019). The second scheme (S2), model freezing, retains the general feature extraction capabilities of the pre-trained model by freezing all layers except the final one, allowing only the last layer to be fine-tuned to the target domain (Basha et al., 2021; Zunair et al., 2018). This approach is particularly beneficial when the pre-trained model already captures robust generalizable features. The third scheme (S3), full fine-tuning with initialization, follows the same process as full fine-tuning but differs in its initialization strategy (de Lima Mendes et al., 2021; Hua et al., 2023;

Table 1

Dataset overview encompassing summary statistics (2012–2023) of output and input features, along with the number of monitoring sites and sample sizes. Ranges and medians were calculated based on measured values in the dataset for each river.

Category	River	Nakdong River	Han River	Geum River	Yeongsan River
	Variable (unit)	Range (Median)	Range (Median)	Range (Median)	Range (Median)
Biological	Cyanobacteria cell counts (cells/mL)	0–750,026 (175)	0–16,823 (0)	0–265,485 (0)	0–220,350 (0)
Water quality	Chlorophyll-a (mg/L)	0.40–150.40 (16.00)	0.10–153.70 (8.20)	1.10–225.55 (27.30)	0.80–238.50 (41.10)
	Total phosphorus (mg/L)	0.000–0.493 (0.034)	0.005–0.772 (0.036)	0.017–0.558 (0.065)	0.020–0.888 (0.126)
	Total nitrogen (mg/L)	0.080–7.275 (2.566)	1.148–13.185 (2.676)	1.346–8.150 (3.317)	1.514–13.960 (4.509)
	Water temperature (°C)	0.30–34.10 (18.10)	0.10–32.10 (15.85)	0.50–32.10 (16.30)	2.30–33.70 (17.85)
Meteorological	Air temperature (°C)	−8.17–31.23 (15.08)	−11.34–32.09 (13.99)	−9.19–31.89 (14.23)	−5.30–30.86 (15.01)
	Precipitation (mm)	0.00–453.95 (6.10)	0.00–407.90 (6.05)	0.00–503.05 (7.05)	0.00–650.30 (9.15)
	Forecast temperature (°C)	−1.47–35.84 (20.34)	−1.47–35.84 (20.21)	−1.47–35.84 (20.17)	−1.47–35.84 (20.13)
Hydrological	Water level (EL.m)	2.22–158.25 (25.52)	0.00–141.40 (33.04)	1.12–77.07 (8.71)	−1.41–7.68 (3.61)
	Total discharge (m ³ /s)	0.00–38,151.22 (540.33)	0.00–69,190.63 (883.03)	0.00–28,553.22 (384.67)	0.00–12,489.44 (152.90)
	Number of sites	12	9	3	2
	Number of observations	5902	4189	1777	1210

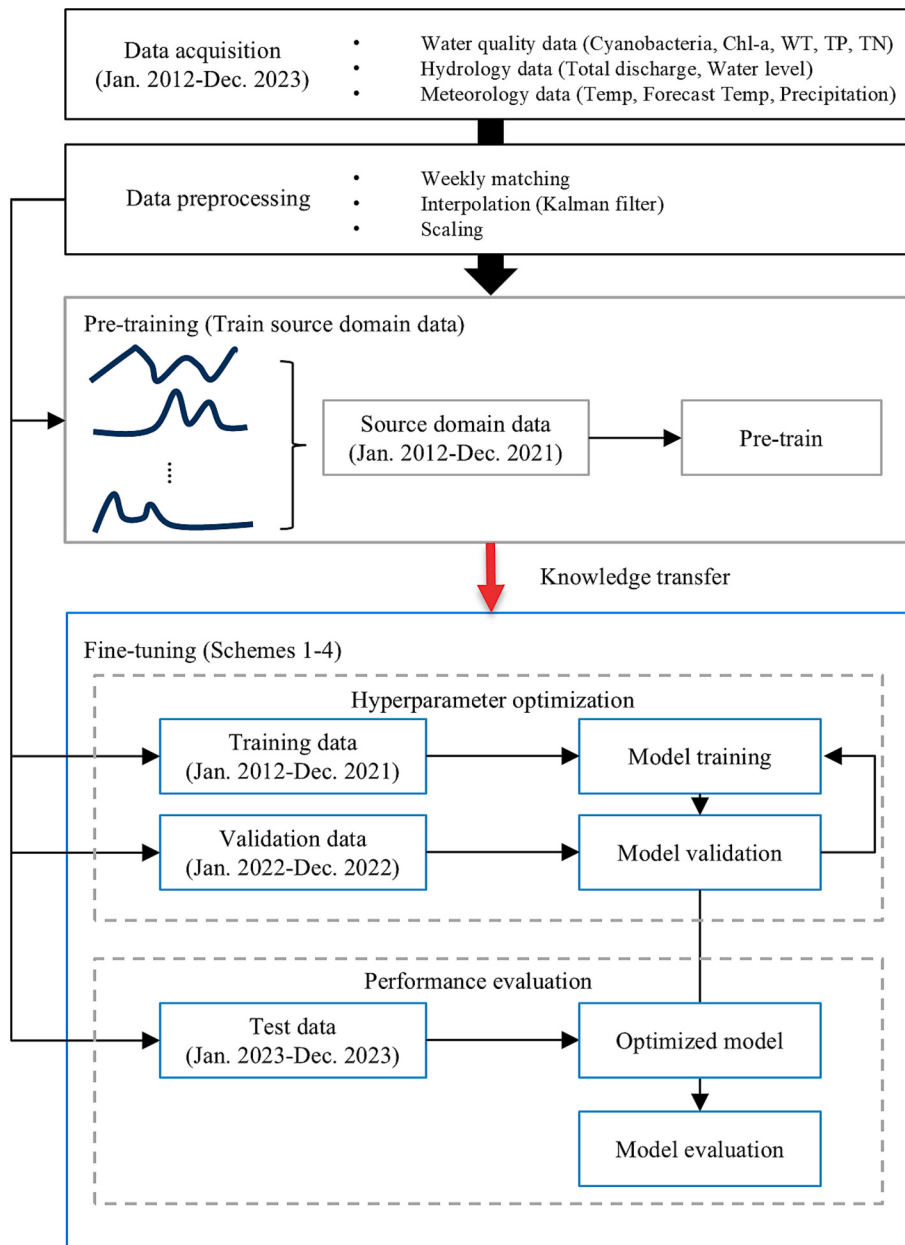


Fig. 2. Schematic diagram of the modeling procedure employing various transfer learning schemes for forecasting harmful algal blooms.

(Nagae et al., 2022). Instead of updating all model parameters directly, this scheme first initializes the weights of the final layer before conducting fine-tuning. This initialization allows the model to adapt more effectively to site-specific characteristics while retaining knowledge from pre-training. Lastly, the fourth scheme (S4), model freezing with initialization combines both model freezing and parameter initialization by keeping all layers frozen except for the final layer, which is initialized before fine-tuning. This approach balances knowledge retention and task-specific adaptation, ensuring that the pre-trained feature extraction remains robust while enabling the output layer to adjust to the target site. By systematically evaluating different TL schemes, this study aims to improve model adaptability across multiple monitoring sites and provide insights into the effectiveness of TL in environmental forecasting.

2.2.2. Implementation of DL models for HAB forecasting

To generalize the applicability of TL in HAB forecasting, six DL models were employed: LSTM, Bi-LSTM, GRU, CLA, Transformer, and

TFT. Missing values in time-series data were interpolated using the Kalman filter to ensure temporal consistency. Cyanobacteria cell counts, the model output, were aligned with environmental data weekly. Since the cyanobacteria cell counts are typically measured weekly but increase to twice per week when exceeding the Warning level ($\geq 10,000$ cells/mL), their mean was used for those weeks before interpolation.

Only observed (non-interpolated) values were used for loss computation during training, validation, and test. The dataset was divided into training (Jan 2012–Dec 2021), validation (Jan 2022–Dec 2022), and test (Jan 2023–Dec 2023) periods, with training start years varying by site due to data availability. To further assess the effectiveness of TL in data-scarce conditions, fine-tuning using only data from the year 2021 was conducted along with the full training dataset (2012–2021). In both cases, pretraining was conducted on the full source domain dataset. This comparison aimed to evaluate the additional benefits of TL when applied to extremely limited target domain data. Cyanobacteria cell counts were transformed using the common logarithm and input variables were min-max normalized using training set to prevent data

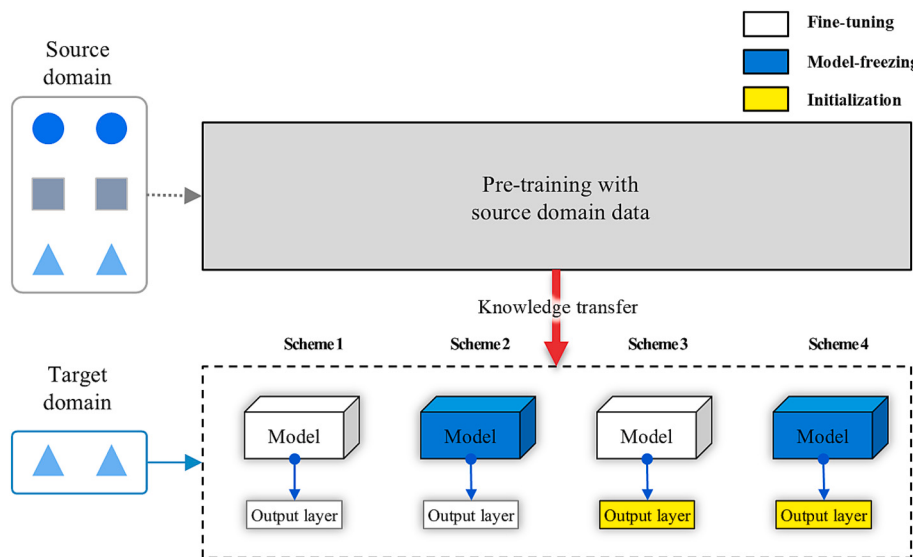


Fig. 3. Transfer learning schemes used in this study. Scheme 1: full fine-tuning, Scheme 2: model-freezing, Scheme 3: full fine-tuning with initialization, and Scheme 4: model-freezing with initialization.

leakage. The forecasting horizon was set to one week to align with the weekly monitoring cycle of the Harmful Algal Bloom Alert System of South Korea, providing a practically relevant lead time for management actions. The input sequence length was determined as two weeks, which was found to be most suitable for capturing short-term bloom dynamics in preliminary experiments with longer sequences (4, 12, and 24 weeks). While longer input windows provided additional context, the two-week configuration offered the best balance between capturing temporal patterns and maintaining forecasting stability.

Model training employed the Adam optimizer, with hyperparameter tuning via grid search. The batch size (4–32), initial learning rate (0.001–0.0001), and dropout (0.0–0.4) were tuned to optimize model performance. Learning rate scheduler was used to gradually reduce the learning rate when the loss stagnated to ensure that models achieve stable convergence during training, while early stopping was applied to prevent overfitting. The TFT model used quantile loss (Lim et al., 2019), while other models used mean squared error (MSE) loss. Other hyperparameters were individually optimized (Table S1).

Forecast air temperature and a seasonal categorical variable (November–May and June–October) were included as inputs. The TFT model processed them as known inputs and static covariates, respectively, while other models treated them as standard features, using the seven-day average air temperature corresponding to each cyanobacteria abundance measurement date.

For source domain dataset construction, monitoring sites with excessive missing data (four from the Nakdong River and two from the Han River) were excluded to maintain pretraining quality. The dataset, concatenated to preserve time-series continuity, contained 10,119 samples. Pretrained models were transferred to 26 monitoring sites for generalization assessment.

All models were trained for 200 epochs during pretraining and initial training before TL, which was limited to 50 epochs during fine-tuning to prevent overfitting. This framework enables models to leverage pretrained knowledge while adapting to site-specific conditions. All training was performed under identical computational conditions to ensure that performance differences reflect methodological factors rather than hardware settings. DL models and TL schemes were implemented in Python 3.11.5 using PyTorch 2.0.1 for model development and training, Scikit-learn 1.3.0 for preprocessing and evaluation, and pykalman 0.9.7 for Kalman filter interpolation.

2.2.3. Performance evaluation

To evaluate the HAB forecasting performance of the DL models integrated with various TL schemes, three evaluation metrics were computed on the test sets: coefficient of determination (R^2), root mean squared error (RMSE), and mean absolute error (MAE).

2.3. Variable importance analysis for HAB forecasting

To improve the interpretability of model outputs and to identify the key drivers of HAB forecasting, variable importance was assessed based on SHapley Additive exPlanations (SHAP). SHAP is a game-theoretic framework that quantifies the marginal contribution of each input variable to the model prediction (Lundberg and Lee, 2017). In this study, the analysis was performed within the Temporal Fusion Transformer (TFT), which demonstrated the most robust forecasting performance among the tested models. For each monitoring site, SHAP values were computed using the best-performing TL scheme to identify the variables with the greatest influence on forecasted cyanobacterial abundance.

To obtain an overall measure of variable importance, the mean absolute SHAP value was calculated across all samples for each input feature. This approach provides a global ranking of variables by quantifying their average contribution to the model predictions, thereby enabling consistent comparison of the relative importance of biological, water quality, hydrological, meteorological, and static covariates across various monitoring sites.

3. Results & discussion

3.1. Spatiotemporal variability of HABs and implications for forecasting

During the study period (2012–2023), the Nakdong River exhibited the highest cyanobacteria cell counts, reaching a maximum of 750,026 cells/mL, followed by the Geum River (265,485 cells/mL) and the Yeongsan River (220,350 cells/mL), while the Han River (16,823 cells/mL) consistently showed relatively low cyanobacterial abundance (Table 1). Despite these high peak values, median cyanobacterial cell counts were zero across all rivers except the Nakdong River, indicating that blooms were sporadic and largely confined to specific seasons (Fig. 4). Cyanobacterial abundance generally increased downstream across all river systems, with cyanobacteria cell counts rising from upstream to downstream sites (Kim et al., 2019; Shin et al., 2017). Seasonal analysis revealed that the majority of blooms occurred during the

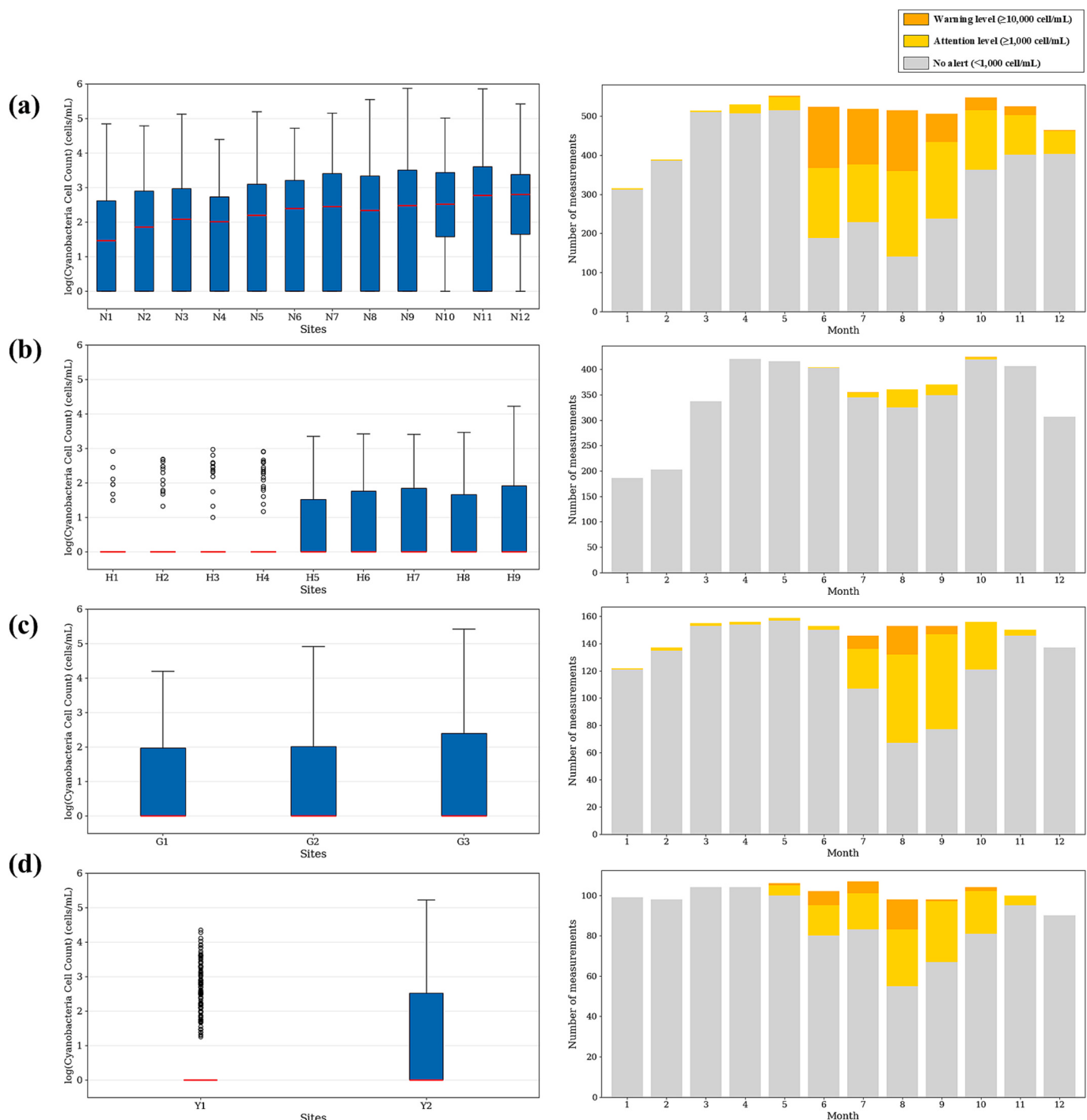


Fig. 4. Box plots of cyanobacteria cell counts and corresponding measurement frequencies across different alert levels (No alert, Attention level, and Warning level) in the Harmful Algal Bloom Alert System for four major rivers in South Korea: (a) Nakdong River, (b) Han River, (c) Geum River, and (d) Yeongsan River. For each river, sites are arranged from upstream (left) to downstream (right) over the 2012–2023 period. Left panels show cyanobacteria cell counts, and right panels show the number of measurements by alert level. Colors indicate alert levels: gray (No alert), yellow (Attention level), and orange (Warning level). (For interpretation of the references to colour in this figure legend, the reader is referred to the web version of this article.)

summer (June–August) and fall (September–November) months (Kim et al., 2022; Kim et al., 2023; Shin and Cha, 2025). Across all rivers, 92.44 %–100.00 % of cyanobacterial blooms exceeding the Attention Level (1000 cells/mL) and 96.88 %–100.00 % of those surpassing the Warning Level (10,000 cells/mL) were recorded during this period. Notably, in the Nakdong and Geum Rivers, cyanobacterial blooms persisted beyond the typical bloom season, extending into the winter months (December–February), suggesting prolonged bloom occurrences

in these systems (Fig. 4a, c).

Advanced DL models, particularly Transformer-based models that extend beyond traditional RNN-based approaches, can be employed to more effectively capture complex temporal dependencies when sufficient training data are available. Previous studies have demonstrated their superior adaptability as Transformer-based architectures outperformed RNNs in various environmental forecasting applications (Demiray et al., 2025; Xu et al., 2023). These characteristics emphasize

the importance of employing TL-based approaches, which are capable of leveraging information from data-rich sites and are particularly valuable for HAB forecasting under pronounced variability. Building on this rationale, the following sections empirically evaluate TL effectiveness across multiple DL models, HAB site conditions, and variation in target domain sample size.

3.2. Impact of TL integration on DL forecasting performance

Forecasting performance was evaluated at 26 cyanobacteria monitoring sites across four major rivers using six DL models—TFT, Transformer, CLA, LSTM, Bi-LSTM, and GRU—and four TL schemes (S1–S4). Four sites in the Han River (H1–H4) were excluded from the evaluation due to consistently low cyanobacteria cell counts (near zero) during the test period. Overall, TL improved forecasting performance across all DL models and schemes (Table 2, Table 3). Pre-TL, the average R^2 across all sites and models ranged from 0.35 to 0.50, indicating moderate predictive accuracy. Post-TL, the average R^2 increased to 0.47–0.60, demonstrating the effectiveness of TL in enhancing forecasting performance. When considering only the best-performing scheme at each site, R^2 values ranged from 0.23 to 0.89 for TFT, 0.27–0.86 for Transformer, 0.26–0.88 for CLA, 0.19–0.87 for LSTM, 0.25–0.85 for Bi-LSTM, and 0.21–0.85 for GRU. These results indicate that TL enabled certain models to reach high predictive accuracy at particular sites, despite the overall average performance remaining moderate. In terms of the number of sites where each model achieved the best post-TL performance, TFT outperformed others at 11 sites, followed by Transformer model at 6, CLA at 4, and Bi-LSTM at 1. Detailed performance metrics, including RMSE and MAE, are presented in Table S2 and Table S3.

While all DL models benefited from TL, performance varied across architecture (Table 2, Table 3). Among the models, TFT most consistently achieved the highest forecasting accuracy across sites as dataset size increased. Their ability to capture long-range dependencies and process heterogeneous temporal data through self-attention mechanisms likely contributed to this advantage, consistent with findings from

recent environmental forecasting studies (Demiray et al., 2025; Xu et al., 2023). CLA model achieved the highest performance pre-TL, outperforming others in the initial training phase (Table 2, Fig. 6). However, its post-TL improvements were relatively modest, as the model had already maximized its feature extraction capability prior to TL, resulting in limited additional gains post-TL. Despite this, CLA consistently outperformed traditional RNN-based models (LSTM, Bi-LSTM, and GRU) across multiple sites, highlighting the advantages of integrating convolutional layers and attention mechanisms. Within the RNN-based models, LSTM exhibited the greatest post-TL improvement, largely due to its initially lower pre-TL performance. Nevertheless, its overall performance remained inferior to that of Transformer-based models, suggesting that although TL can partially offset the limitations of RNNs, but not fully overcome fundamental architectural constraints, such as inefficiencies in sequential processing.

Notably, prior HAB forecasting studies have primarily applied TL to RNN-based models, particularly LSTMs (Ni et al., 2022), while Transformer-based architectures remain underexplored. This study presents the first systematic application of TL using Transformer models in HAB forecasting, demonstrating their superior adaptability—especially in data-rich conditions. Given their robust performance and scalability, Transformer-based models should be prioritized in future HAB forecasting efforts as data availability continues to expand. Their strong generalization across monitoring sites further positions them as a preferred choice for developing reliable forecasting and early warning systems.

3.3. River-specific TL performance under varying bloom intensity and data richness

The application of TL improved forecasting performance across all river systems, with the degree of enhancement varying according to river-specific characteristics (Table 4, Fig. 5). In all cases, R^2 increased by 12.51 %–82.49 %, while RMSE and MAE decreased by 4.39 %–27.99 % and 0.12 %–29.87 %, respectively, demonstrating consistent

Table 2

Comparison of forecasting performance for harmful algal blooms using R^2 across different transfer learning (TL) schemes and sites for the TFT, Transformer, and CLA models. S1–S4 denote TL schemes with varying levels of parameter adaptation (see Fig. 3 for details), while S0 indicates the baseline model without TL. Bolded values represent the highest R^2 achieved among the TL schemes for each model-site combination, and colored values indicate the best overall performance among all DL models for each site. Sites H1–H4 are excluded due to extremely low cyanobacterial cell counts during the test period. Site initials correspond to river systems: N = Nakdong, H = Han, G = Geum, Y = Yeongsan.

Model	TFT						Transformer						CLA			
	Scheme						Scheme						Scheme			
Site	S0	S1	S2	S3	S4	S0	S1	S2	S3	S4	S0	S1	S2	S3	S4	
N1	0.43	0.59	0.50	0.64	0.48	0.46	0.51	0.51	0.53	0.50	0.48	0.61	0.53	0.59	0.45	
N2	0.49	0.61	0.34	0.62	0.49	0.47	0.57	0.52	0.56	0.55	0.59	0.64	0.61	0.60	0.55	
N3	0.70	0.80	0.75	0.76	0.71	0.71	0.79	0.80	0.80	0.79	0.77	0.82	0.80	0.76	0.79	
N4	0.49	0.72	0.63	0.55	0.62	0.60	0.70	0.64	0.68	0.59	0.59	0.71	0.67	0.64	0.47	
N5	0.65	0.76	0.56	0.71	0.69	0.61	0.69	0.70	0.68	0.62	0.65	0.71	0.71	0.70	0.70	
N6	0.66	0.78	0.71	0.71	0.69	0.57	0.67	0.63	0.75	0.59	0.66	0.72	0.57	0.73	0.54	
N7	0.59	0.83	0.77	0.82	0.77	0.62	0.73	0.78	0.81	0.78	0.69	0.79	0.78	0.63	0.67	
N8	0.66	0.78	0.68	0.79	0.70	0.67	0.79	0.73	0.78	0.73	0.69	0.76	0.69	0.74	0.51	
N9	0.79	0.89	0.84	0.85	0.84	0.74	0.84	0.78	0.81	0.77	0.78	0.88	0.85	0.84	0.73	
N10	0.50	0.64	0.57	0.65	0.54	0.49	0.55	0.53	0.51	0.64	0.57	0.61	0.50	0.53	0.43	
N11	0.61	0.74	0.67	0.64	0.65	0.59	0.70	0.71	0.76	0.65	0.60	0.74	0.70	0.68	0.60	
N12	0.45	0.68	0.68	0.70	0.64	0.51	0.59	0.71	0.64	0.66	0.36	0.61	0.50	0.43	0.22	
H5	0.41	0.46	0.34	0.52	0.45	0.41	0.50	0.44	0.40	0.58	0.46	0.36	0.39	0.49	0.35	
H6	0.30	0.33	0.29	0.41	0.31	0.33	0.34	0.42	0.38	0.42	0.25	0.32	0.33	0.17	0.14	
H7	0.06	0.01	-0.06	0.21	0.23	0.12	0.17	0.24	0.18	0.31	0.12	0.15	0.21	0.12	0.26	
H8	0.20	0.31	0.46	0.32	0.36	0.25	0.41	0.31	0.42	0.31	0.23	0.31	0.38	0.31	0.41	
H9	0.25	0.60	0.44	0.49	0.43	0.40	0.47	0.56	0.47	0.57	0.41	0.59	0.54	0.50	0.43	
G1	0.03	0.26	0.28	0.26	0.25	0.03	0.05	0.07	0.13	0.27	0.11	0.25	0.29	0.16	0.23	
G2	0.56	0.65	0.65	0.78	0.66	0.54	0.68	0.64	0.68	0.69	0.41	0.77	0.63	0.75	0.51	
G3	0.66	0.83	0.75	0.81	0.72	0.51	0.86	0.74	0.85	0.74	0.69	0.77	0.69	0.86	0.65	
Y1	0.38	0.49	0.42	0.54	0.34	0.35	0.63	0.52	0.61	0.52	0.53	0.57	0.43	0.60	0.42	
Y2	0.31	0.33	0.16	0.36	0.22	0.48	0.52	0.48	0.58	0.57	0.37	0.45	0.36	0.39	0.29	
Avg.	0.46	0.60	0.52	0.60	0.54	0.48	0.58	0.57	0.59	0.58	0.50	0.60	0.55	0.56	0.47	
# Best (post-TL)	11									6					4	

Table 3

Comparison of forecasting performance for harmful algal blooms using R^2 across different transfer learning (TL) schemes and sites for the LSTM, Bi-LSTM, and GRU models. S1–S4 denote TL schemes with varying levels of parameter adaptation (see Fig. 3 for details), while S0 indicates the baseline model without TL. Bolded values represent the highest R^2 achieved among the TL schemes for each model-site combination, and colored values indicate the best overall performance among all DL models for each site. Sites H1–H4 are excluded due to extremely low cyanobacterial cell counts during the test period. Site initials correspond to river systems: N = Nakdong, H = Han, G = Geum, Y = Yeongsan.

Model	LSTM					Bi-LSTM					GRU				
	Scheme		Scheme			Scheme		Scheme			Scheme			Scheme	
Site	S0	S1	S2	S3	S4	S0	S1	S2	S3	S4	S0	S1	S2	S3	S4
N1	0.33	0.51	0.47	0.60	0.48	0.46	0.54	0.55	0.59	0.55	0.46	0.59	0.59	0.48	0.57
N2	0.32	0.61	0.56	0.57	0.52	0.41	0.55	0.51	0.55	0.46	0.46	0.58	0.52	0.54	0.52
N3	0.38	0.81	0.79	0.80	0.79	0.67	0.78	0.77	0.78	0.77	0.65	0.78	0.77	0.79	0.75
N4	0.55	0.71	0.69	0.64	0.67	0.56	0.70	0.67	0.68	0.66	0.61	0.70	0.66	0.70	0.65
N5	0.51	0.70	0.71	0.67	0.71	0.65	0.69	0.73	0.70	0.74	0.65	0.70	0.71	0.68	0.71
N6	0.38	0.75	0.62	0.75	0.57	0.67	0.77	0.68	0.76	0.68	0.62	0.74	0.70	0.71	0.55
N7	0.39	0.79	0.78	0.78	0.79	0.67	0.77	0.78	0.74	0.79	0.74	0.79	0.78	0.82	0.75
N8	0.29	0.68	0.64	0.69	0.35	0.66	0.73	0.71	0.74	0.70	0.69	0.75	0.73	0.71	0.73
N9	0.25	0.80	0.85	0.87	0.84	0.77	0.85	0.84	0.84	0.84	0.76	0.85	0.85	0.85	0.78
N10	0.23	0.39	0.52	0.49	0.52	0.47	0.64	0.50	0.41	0.49	0.49	0.61	0.43	0.53	0.32
N11	0.10	0.27	0.23	0.36	0.19	0.61	0.81	0.69	0.77	0.69	0.57	0.70	0.67	0.65	0.63
N12	0.54	0.68	0.61	0.56	0.37	0.52	0.68	0.59	0.64	0.57	0.34	0.64	0.66	0.45	0.35
H5	0.42	0.44	0.39	0.45	0.39	0.42	0.37	0.42	0.34	0.42	0.42	0.34	0.39	0.37	0.40
H6	0.34	0.34	0.36	0.38	0.36	0.28	0.33	0.35	0.26	0.32	0.26	0.32	0.37	0.26	0.35
H7	0.07	0.22	0.20	0.17	0.20	0.16	0.20	0.19	0.23	0.27	0.11	0.21	0.14	0.15	0.20
H8	0.29	0.38	0.34	0.30	0.30	0.21	0.42	0.32	0.31	0.31	0.19	0.28	0.37	0.23	0.38
H9	0.44	0.52	0.37	0.45	0.38	0.43	0.51	0.53	0.50	0.45	0.44	0.51	0.44	0.50	0.43
G1	0.07	0.16	0.19	0.16	0.07	0.12	0.21	0.25	0.24	0.17	0.12	0.17	0.19	0.21	0.16
G2	0.53	0.74	0.61	0.75	0.59	0.42	0.74	0.74	0.68	0.50	0.49	0.71	0.60	0.69	0.60
G3	0.61	0.86	0.81	0.85	0.79	0.68	0.80	0.75	0.82	0.75	0.64	0.77	0.74	0.68	0.73
Y1	0.38	0.46	0.51	0.62	0.49	0.39	0.50	0.46	0.46	0.43	0.38	0.48	0.42	0.40	0.36
Y2	0.37	0.46	0.32	0.42	0.31	0.34	0.39	0.32	0.39	0.27	0.33	0.43	0.30	0.40	0.30
Avg.	0.35	0.56	0.53	0.56	0.49	0.48	0.59	0.56	0.57	0.53	0.47	0.58	0.55	0.54	0.51
# Best (post-TL)		0					1					0			

Table 4

Forecasting performance for harmful algal blooms across different rivers, comparing results without transfer learning (S0) and with transfer learning (TL). The best-performing TL scheme is marked, and percentage improvements following TL are also indicated.

Model	River	Nakdong River			Han River			Geum River			Yeongsan River		
		Metric	R ²	RMSE	MAE	R ²	RMSE	MAE	R ²	RMSE	MAE	R ²	RMSE
TFT	S0	0.59	0.90	0.68	0.25	0.88	0.61	0.42	1.05	0.54	0.35	1.10	0.65
	+TL	0.73	0.71	0.48	0.39	0.79	0.54	0.62	0.83	0.44	0.45	1.06	0.61
Transformer	Improved	25.53 %	20.81 %	29.87 %	59.44 %	10.55 %	11.06 %	47.19 %	20.77 %	18.87 %	28.83 %	3.91 %	6.53 %
	S0	0.59	0.90	0.72	0.30	0.85	0.62	0.36	1.12	0.72	0.41	1.07	0.69
CLA	Improved	17.86 %	14.78 %	14.26 %	44.35 %	10.56 %	6.77 %	57.15 %	20.70 %	19.86 %	43.43 %	15.65 %	18.69 %
	S0	0.62	0.86	0.69	0.29	0.85	0.66	0.40	1.07	0.74	0.45	1.05	0.69
LSTM	Improved	15.79 %	14.17 %	18.86 %	25.66 %	5.78 %	4.97 %	49.01 %	21.85 %	24.38 %	12.51 %	5.41 %	10.62 %
	S0	0.35	1.13	0.93	0.31	0.84	0.65	0.41	1.07	0.77	0.37	1.12	0.75
Bi-LSTM	Improved	82.49 %	27.99 %	29.17 %	21.63 %	5.04 %	4.22 %	44.73 %	21.37 %	25.68 %	39.51 %	11.69 %	15.63 %
	S0	0.59	0.89	0.71	0.30	0.85	0.65	0.41	1.07	0.73	0.36	1.13	0.76
GRU	Improved	19.79 %	15.94 %	17.75 %	23.42 %	5.39 %	7.89 %	43.50 %	18.96 %	21.50 %	22.54 %	6.29 %	6.30 %
	S0	0.59	0.89	0.73	0.28	0.85	0.64	0.42	1.06	0.72	0.35	1.14	0.77
	+TL	0.70	0.76	0.61	0.35	0.82	0.64	0.55	0.91	0.61	0.45	1.05	0.72
	Improved	20.01 %	15.29 %	16.59 %	23.27 %	4.39 %	0.12 %	31.28 %	14.54 %	15.50 %	29.20 %	8.20 %	6.84 %

performance gains post-TL across all rivers. The extent of improvement was closely related to cyanobacterial abundance.

The Nakdong River, which exhibited the highest mean cyanobacterial cell counts, had pre-TL R^2 values of 0.35–0.62, which increased to 0.64–0.73 post-TL, reflecting improvements of 15.79 %–82.49 %. The relatively persistent high cell counts in the Nakdong River provided richer temporal patterns for model learning, enabling more effective capture of bloom dynamics and stronger forecasting performance. This was further supported by marked reductions in RMSE (14.17 %–27.99 %) and MAE (14.26 %–29.87 %), indicating that TL not only enhanced explanatory power but also reduced absolute prediction errors, making forecasts more reliable for management purposes. Similarly, the Geum

and Yeongsan Rivers, both with moderate cell counts, showed pre-TL R^2 values of 0.36–0.42 and 0.35–0.45, respectively. Post-TL, R^2 improved to 0.55–0.62 in the Geum and 0.44–0.59 in the Yeongsan, corresponding to improvements of 31.28 %–57.15 % and 12.51 %–28.83 %, respectively.

In contrast, the Han River, characterized by the lowest HAB occurrences, exhibited the weakest forecasting performance among the four rivers. Pre-TL forecasting performance ($R^2 = 0.25$ –0.31) still benefited from TL, achieving post-TL R^2 values of 0.35–0.44 (21.63 %–59.44 % improvement). Although RMSE (4.39 %–10.56 %) and MAE (0.12 %–11.06 %) also decreased, the reductions were modest compared to high-bloom rivers. The particularly small reduction in MAE reflects that

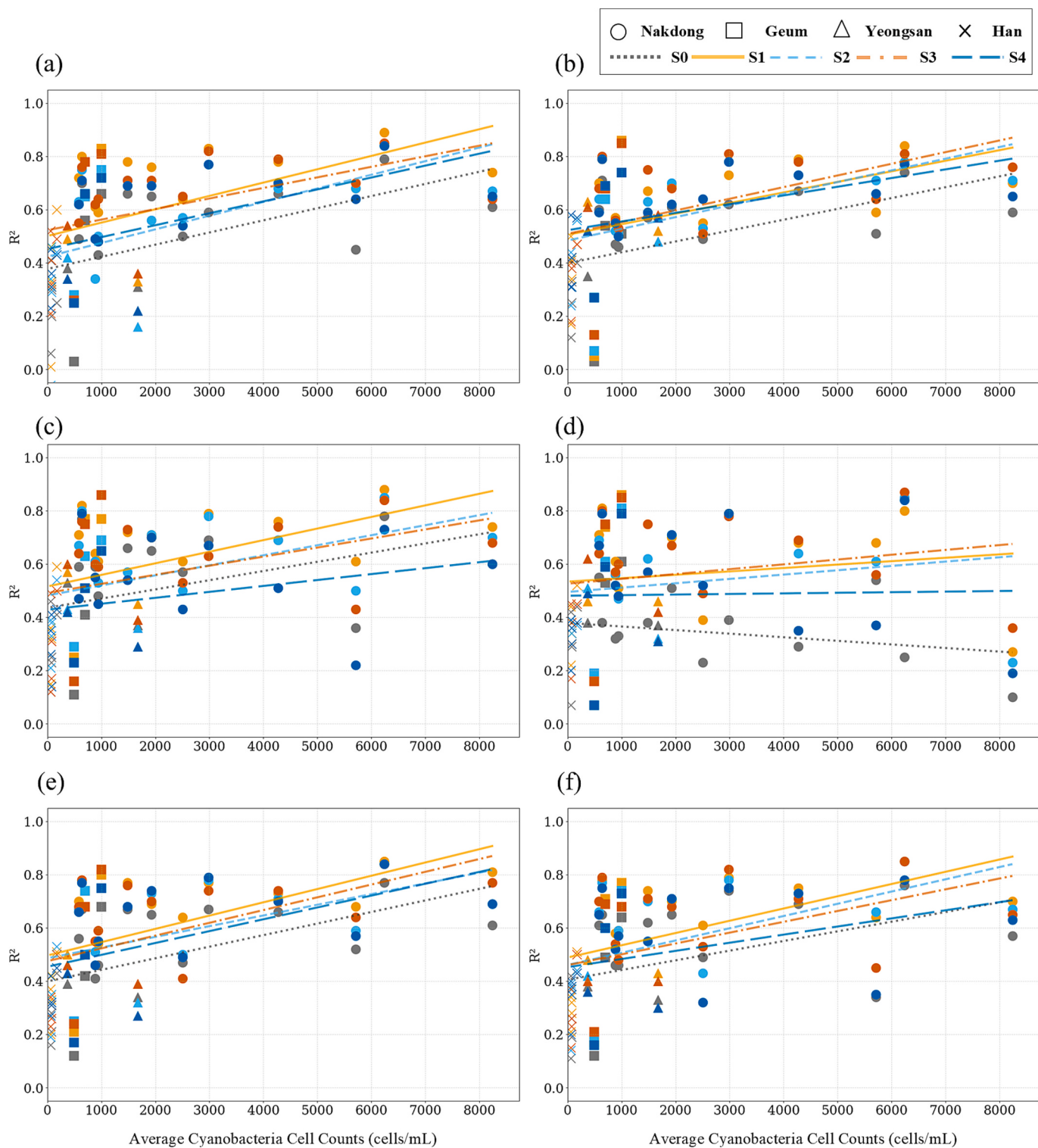


Fig. 5. Effects of the average cyanobacteria cell count per monitoring site on test performance using R^2 across different transfer learning (TL) schemes (S1–S4) and deep learning models: (a) TFT, (b) Transformer, (c) CLA, (d) LSTM, (e) Bi-LSTM, and (f) GRU. Lines represent linear regression trends for different TL schemes, with colors indicating the schemes (S0: gray, S1: yellow, S2: sky blue, S3: orange, S4: blue). (For interpretation of the references to colour in this figure legend, the reader is referred to the web version of this article.)

average errors were already low due to the scarcity of bloom events, leaving limited potential for further improvement. In contrast, RMSE—being more sensitive to rare but large deviations—showed relatively greater reductions, suggesting that TL mainly improved the model's ability to capture occasional bloom peaks rather than reducing errors during non-bloom periods. Beyond metric difference, this

relatively modest improvement was also partly due to sparse bloom occurrence and a limited number of designated water quality monitoring sites, which constrained the availability of informative temporal patterns for model learning. While TL partially offset data scarcity by transferring knowledge from data-rich regions, its effectiveness was constrained by limited variability and weaker site-specific patterns,

which restricted post-TL performance.

Overall, these results indicate that sites with higher cyanobacterial abundance and richer temporal patterns generally exhibited stronger forecasting performance (R^2 , RMSE, MAE), both pre- and post-TL. Although TL can substantially improve performance in data-scarce environments, its effectiveness is reduced when local patterns are insufficiently represented. This underscores that the effectiveness of TL depends not only on cross-site knowledge transfer but also on the richness of local patterns and highlights the complementary value of different performance metrics in evaluating model improvements under contrasting bloom conditions.

3.4. Impact of TL scheme selection and implications for TL optimization

The forecasting performance of each TL scheme was evaluated based on the average R^2 across all sites for each model and the number of sites where each scheme achieved the best performance (Table 2, Table 3, Fig. 6). On average, S1 (0.56–0.60) and S3 (0.54–0.60) outperformed S2 (0.53–0.56) and S4 (0.47–0.58). S1 achieved the highest number of best-performing sites (57), followed by S3 (39), S2 (17), and S4 (16). S1 was most effective for TFT, Transformer, and GRU, while S3 performed best with CLA, LSTM, and Bi-LSTM. In models where S3 ranked highest at multiple sites, the number of best-performing sites under S1 and S3 was comparable, suggesting that both schemes were competitive in adapting to site-specific conditions. These differences reflect the degree of parameter tuning, with S1 involving full fine-tuning, while S2 and S4 employed extensive parameter freezing, limiting model adaptability.

Overall, full fine-tuning approaches (S1, S3) generally outperformed model-freezing methods (S2, S4) across a larger number of sites (Fig. 6). Among them, S1 most frequently achieved the highest forecasting performance, demonstrating the advantages of fully adapting the model to the fine-tuning site. Allowing the entire model to adjust appears to enhance predictive accuracy by better capturing localized variations in HAB dynamics. In contrast, model-freezing approaches exhibited limited adaptability, as updating only a subset of layers restricted the ability of the model to learn site-specific patterns. Despite their relatively lower performance, model-freezing schemes are more computationally efficient compared to full fine-tuning, requiring less training time and fewer resources under the same computational environment, an important consideration for real-time or resource-limited applications.

In this study, model-freezing schemes involved fine-tuning only the output layers, which directly influence predictions and are generally

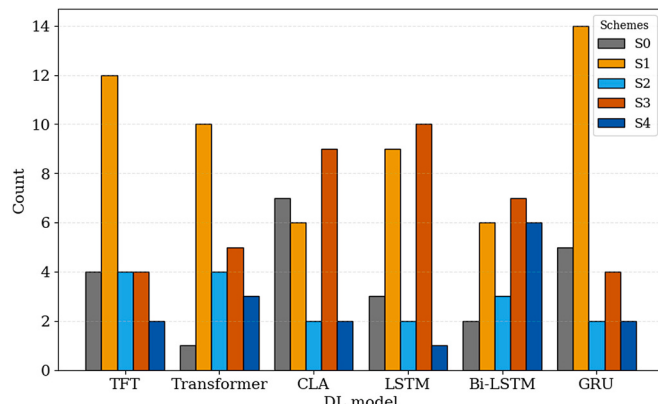


Fig. 6. Comparison of harmful algal bloom forecasting performance without (S0) and with different transfer learning schemes (S1–S4). Bar heights represent the number of best-performing sites across different rivers for each deep learning model. Bar colors indicate the schemes: gray for S0, yellow for S1, sky blue for S2, orange for S3, and blue for S4. (For interpretation of the references to colour in this figure legend, the reader is referred to the web version of this article.)

considered the most transferable across different sites (Basha et al., 2021; Zunair et al., 2018). However, this approach may overlook critical information encoded in earlier layers, reducing the model capacity to adapt to new contexts. Previous research has demonstrated that selectively freezing early and late layers while updating mid-level representations can improve TL performance in time-series forecasting (Ghafoorian et al., 2017). Recent advancements further suggest that adaptive fine-tuning strategies—such as data similarity-based layer selection (Chen et al., 2023), meta-learning-guided tuning (Jang et al., 2019), and optimization-based approaches (Vrbancic and Podgorelec, 2020)—can improve TL effectiveness by automatically determining which layers to freeze or update. These approaches highlight promising directions for further improving the efficiency–accuracy trade-off in TL-based HAB forecasting.

3.5. Impact of target domain sample size and generalization of TL forecasting performance

The best-performing model, TFT, was fine-tuned using only 2021 data per site, with pretraining conducted on the full 2012–2021 dataset to further examine TL generalization under data-scarce conditions. Under full data conditions, TL improved forecasting accuracy across all river systems, with average R^2 values across sites within each river increasing from pre-TL values of 0.24–0.59 to post-TL values of 0.28–0.73 (Fig. 7). When training data was limited to a single year (2021), pre-TL performance declined significantly, with R^2 ranging from –0.17 to 0.34. However, TL effectively mitigated the impact of limited data availability, increasing post-TL R^2 to 0.21–0.70. Across individual rivers, the Nakdong and Geum Rivers showed the greatest post-TL improvements under both data conditions, with R^2 increasing from pre-TL values of 0.34 to post-TL values of 0.53–0.70 in the Nakdong River and from –0.17 to 0.39–0.53 in the Geum River. The Yeongsan River also showed considerable improvements, with R^2 increasing from 0.02 to 0.29–0.49. In contrast, the Han River demonstrated more modest gains, with R^2 increasing from 0.03 to 0.21–0.24.

These findings suggest that TL can effectively extract and transfer relevant temporal patterns from environmental time-series data, leading to more accurate and stable forecasting outcomes. Importantly, TL improved forecasting performance in both data-rich and data-scarce regions, underscoring its practical relevance for real-world applications.

From an operational perspective, the capacity of TL to enhance performance with limited data is especially valuable for newly established or under-monitored sites that do not yet possess long-term historical records. By leveraging knowledge from data-rich sites, TL can support the expansion of early warning systems to areas with sparse monitoring networks, enabling more proactive management even in resource-constrained contexts.

3.6. Interpretability of TL-based forecasting models and key drivers of HAB forecasts

The SHAP analysis of the TFT model for the best-performing scheme at each site revealed variables that consistently influenced forecasts across sites, while also capturing site-specific differences in key drivers (Fig. 8). Across sites, cyanobacteria cell counts and meteorological variables—particularly forecast temperature and air temperature—consistently exhibited the highest importance. These findings align with previous studies that link meteorological variability on bloom dynamics (Cha et al., 2017; Elliott, 2012; Paerl and Huisman, 2008; Paerl and Otten, 2013). Among water quality variables, water temperature and TN showed strong influence at multiple sites, while the relative importance of other factors varied depending on local conditions. Hydrological variables generally showed lower importance, though water level was typically more influential than total discharge, suggesting a stronger link between hydraulic retention and bloom persistence. In the Han River, particularly, hydrological variables showed

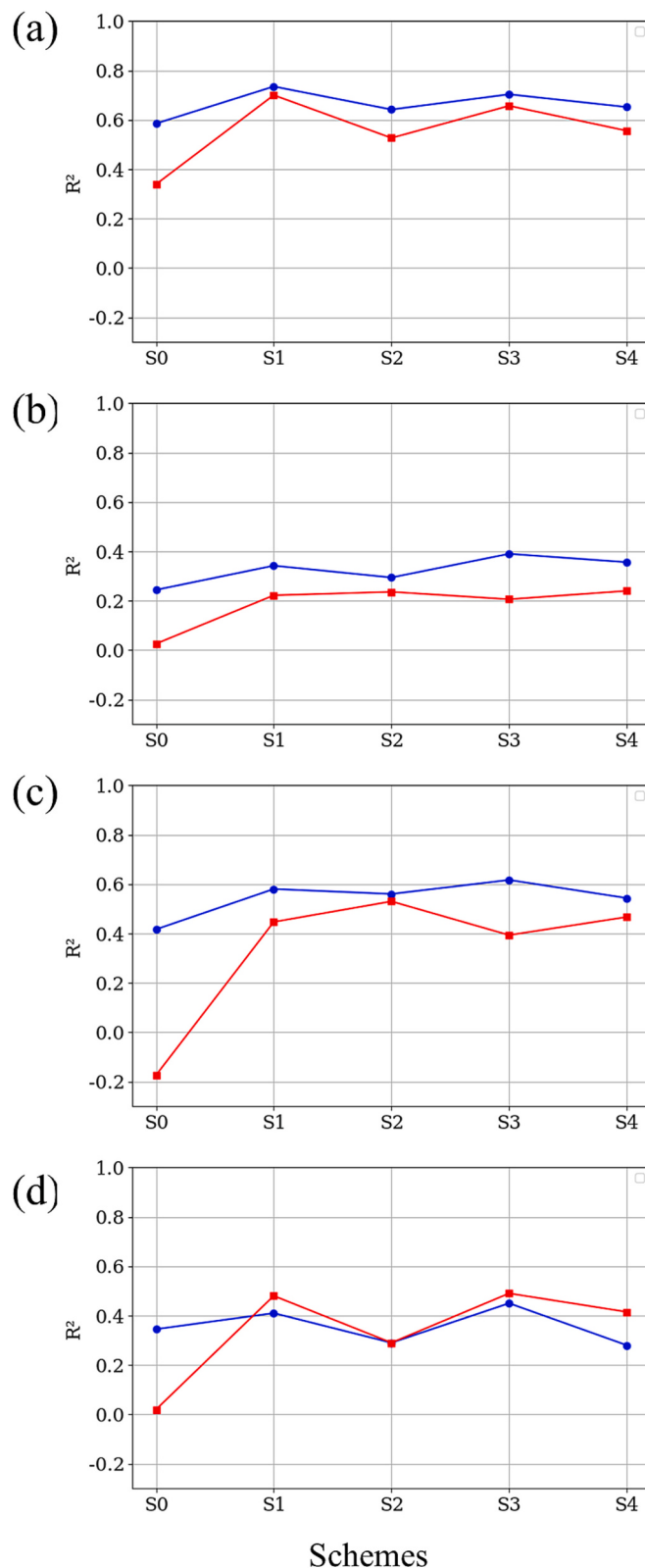


Fig. 7. Effects of target domain sample size on transfer learning performance using R^2 across different rivers: (a) Nakdong River, (b) Han River, (c) Geum River, and (d) Yeongsan River. The blue line represents results obtained using the full dataset (from the start date–2021) for fine-tuning, while the red line represents results using limited training data (2021 only) in the target domain. (For interpretation of the references to colour in this figure legend, the reader is referred to the web version of this article.)

relatively lower importance, likely because no hydraulic structures are directly connected to the monitoring sites and upstream dams are located at considerable distances. “Season” was also identified as important factors at several sites, reflecting the tendency of blooms to peak in summer and fall month.

At 13 sites, cyanobacteria cell counts emerged as the most influential variable, largely because bloom levels remained consistently high from summer into fall, driven by the dominance of *Microcystis* during summer and *Aphanizomenon* from late spring through early winter (Kim et al., 2022; Park et al., 2021). While this persistence explains why cyanobacteria counts frequently outweighed other predictors, it is noteworthy that other variables—including forecast temperature, TN, and water level—still frequently ranked among the top contributors. This indicates that the model captured meaningful patterns from various environmental drivers, which is crucial for representing both bloom initiation and persistence.

The consistency between SHAP-based importance rankings and established ecological understanding suggests that the TL-based TFT model did not rely on spurious correlations but rather identified ecologically and physically meaningful drivers. From a management perspective, the identification of TN and water level as influential predictors highlights controllable factors that can be directly addressed through nutrient reduction measures and hydraulic structure operations. Together, these results underscore both the management relevance of controllable factors and the interpretability of the TL-based forecasting framework, reinforcing its reliability for supporting HAB forecasting and early warning strategies.

3.7. Contribution, limitations, and perspectives of TL-based HABs forecasting

This study makes several key contributions to HAB forecasting. First, it presents the first large-scale and systematic application of TL to Transformer-based architecture, which extends beyond the RNN-based models predominantly used in prior studies. Second, it provides an unprecedented cross-site evaluation across 26 monitoring sites in four major rivers, including both frequent- and rare-bloom sites, to assess the generalizability of TL under diverse and challenging conditions. Third, in contrast to earlier studies that focused on a single transfer strategy, we systematically compared four distinct TL schemes under varying target-domain sample sizes and across six deep learning architecture, providing new insights into their relative effectiveness. Together, these contributions establish a generalizable TL framework that advances the field beyond site-specific case studies and lays a foundation for more reliable, data-scarce HAB forecasting and the development of future operational benchmarks.

Relative to existing approaches, the proposed framework demonstrates stronger adaptability by leveraging Transformer-based models capable of learning heterogeneous temporal dynamics as data availability increases. Nevertheless, several limitations remain. Predictive performance was relatively low at some sites, particularly in the Han River, where bloom events are rare and water quality data are collected only at monthly resolution. At such sites, increasing monitoring frequency or interpolating to higher temporal resolution could provide richer signals and improve model learning. In addition, the predominance of cyanobacteria cell counts among the most important predictors highlights the challenge of capturing both bloom onset and persistence. These represent complementary but distinct forecasting tasks, and future work should explore multi-task learning or mixed-loss strategies that integrate onset classification with abundance regression, thereby capturing both the emergence and progression of blooms.

Despite these limitations, the motivation of this study was not to achieve the highest absolute forecasting accuracy but to demonstrate the relative and generalizable improvements enabled by TL across heterogeneous sites and conditions. With HABs expected to increase in frequency and extent under climate change and anthropogenic pressures,

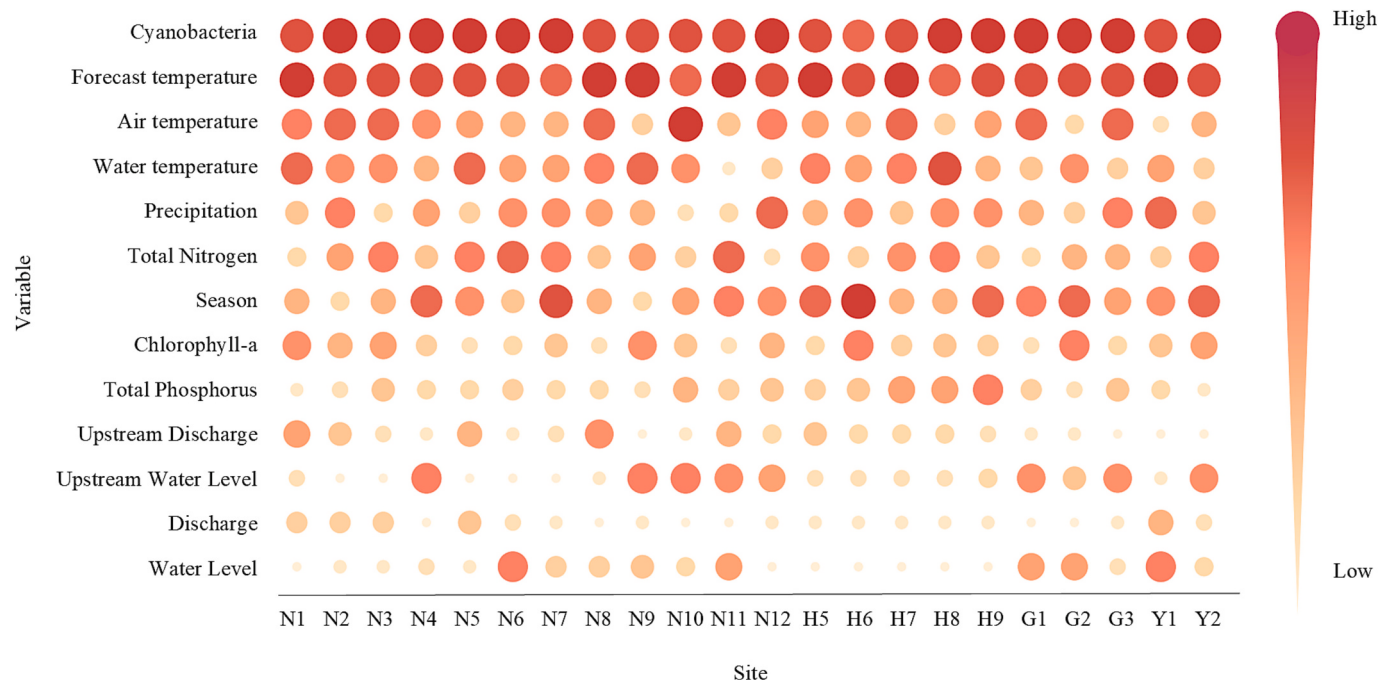


Fig. 8. Site-specific variable importance analysis using SHAP. The plot shows the relative importance of input variables for HAB forecasting in the TFT model, computed under the best-performing TL scheme at each site. Both circle size and colour indicate the relative ranking of SHAP values, with larger and darker circles representing higher importance.

the TL framework presented here provides both a practical baseline for operational forecasting and a foundation for advancing more integrated, context-sensitive HAB prediction systems. Aligning TL implementation with operational needs, including real-time deployment and integration into monitoring programs, will be essential for realizing its full potential in environmental management.

4. Conclusions and future directions

This study demonstrated the effectiveness of TL in enhancing DL-based forecasting of HABs across diverse river systems and monitoring sites in South Korea. By systematically evaluating multiple DL architectures and TL schemes under varying site conditions, the findings confirm that TL consistently improves generalization in data-scarce environments while reducing reliance on extensive site-specific training data. Among the tested schemes, Full fine-tuning emerged as the most effective adaptation strategy, though model-freezing approaches remain promising for computationally constrained scenarios if enhanced through selective layer updating. Incorporating interpretability methods further strengthened confidence in the predictions, underscoring the practical relevance of TL-based forecasting frameworks.

Further research should explore how TL can be more effectively tailored to site-specific conditions and operational constraints. Approaches such as adaptive layer selection, similarity-based source-target matching, or lightweight fine-tuning strategies may help balance performance with computational efficiency. In addition, forecasting bloom onset and bloom persistence represent complementary tasks; future models that combine both could enhance the effectiveness of HAB early-warning systems. More broadly, the TL framework developed in this study provides a transferable modeling strategy for other data-scarce domains in environmental forecasting, supporting scalable and actionable early warning systems under real-world conditions.

Data statement

The data and code used in the study are available at <https://github.com/jp0926/DL-TL.git>

[com/jp0926/DL-TL.git](https://github.com/jp0926/DL-TL.git)

CRediT authorship contribution statement

Jaegwan Park: Writing – original draft, Visualization, Software, Methodology, Data curation. **Taeseung Park:** Software, Methodology, Data curation. **Dogeon Lee:** Investigation, Data curation. **Jihoon Shin:** Methodology, Data curation, Conceptualization. **Kyunghyun Kim:** Funding acquisition, Data curation. **Jonggyu Jung:** Investigation. **Hongtae Kim:** Writing – review & editing, Conceptualization. **Yoon-Kyung Cha:** Writing – review & editing, Project administration, Methodology, Conceptualization.

Declaration of competing interest

The authors declare that they have no known competing financial interests or personal relationships that could have appeared to influence the work reported in this paper.

Acknowledgements

This research was supported by the project “2024 Development of Artificial Intelligence Platform and Water Pollution Accident Analysis System” funded by the National Institute of Environmental Research (NIER), Republic of Korea.

Appendix A. Supplementary data

Supplementary data to this article can be found online at <https://doi.org/10.1016/j.ecoinf.2025.103481>.

Data availability

The data and code used in the study are available at <https://github.com/jp0926/DL-TL.git>.

References

- Ahn, J.M., Kim, J., Kim, H., Kim, K., 2023. Harmful cyanobacterial blooms forecasting based on improved CNN-transformer and temporal fusion transformer. *Environ. Technol. Innov.* 32, 103314. <https://doi.org/10.1016/j.eti.2023.103314>.
- Basha, S.H.S., Vinakota, S.K., Pulabaigari, V., Mukherjee, S., Dubey, S.R., 2021. AutoTune: automatically tuning convolutional neural networks for improved transfer learning. *Neural Netw.* 133, 112–122. <https://doi.org/10.1016/j.neunet.2020.10.009>.
- Burford, M.A., Carey, C.C., Hamilton, D.P., Huisman, J., Paerl, H.W., Wood, S.A., Wulff, A., 2020. Perspective: advancing the research agenda for improving understanding of cyanobacteria in a future of global change. *Harmful Algae* 91, 101601. <https://doi.org/10.1016/j.hal.2019.04.004>.
- Busari, I., Sahoo, D., Das, N., Privette, C., Schlaftzman, M., Sawyer, C., 2025. Advancing harmful algal bloom predictions using chlorophyll-a as an indicator: combining deep learning and EnKF data assimilation method. *J. Environ. Manag.* 382, 125441. <https://doi.org/10.1016/j.jenvman.2025.125441>.
- Carey, C.C., Ibelings, B.W., Hoffmann, E.P., Hamilton, D.P., Brookes, J.D., 2012. Eco-physiological adaptations that favour freshwater cyanobacteria in a changing climate. *Water Res.* 46, 1394–1407. <https://doi.org/10.1016/j.watres.2011.12.016>.
- Carmichael, W.W., 2001. Health effects of toxin-producing cyanobacteria: "The CyanoHABs". *Hum. Ecol. Risk Assess.* 7, 1393–1407. <https://doi.org/10.1080/20018091095087>.
- Cha, Y., Cho, K.H., Lee, H., Kang, T., Kim, J.H., 2017. The relative importance of water temperature and residence time in predicting cyanobacteria abundance in regulated rivers. *Water Res.* 124, 11–19. <https://doi.org/10.1016/j.watres.2017.07.040>.
- Chen, L., Yuan, F., Yang, J., He, X., Li, C., Yang, M., 2023. User-specific adaptive fine-tuning for cross-domain recommendations. *IEEE Trans. Knowl. Data Eng.* 35, 3239–3252. <https://doi.org/10.1109/TKDE.2021.3119619>.
- Chen, S., Huang, J., Wang, P., Tang, X., Zhang, Z., 2024a. A coupled model to improve river water quality prediction towards addressing non-stationarity and data limitation. *Water Res.* 248, 120895. <https://doi.org/10.1016/j.watres.2023.120895>.
- Chen, X., Sun, W., Jiang, T., Ju, H., 2024b. Enhanced prediction of river dissolved oxygen through feature- and model-based transfer learning. *J. Environ. Manag.* 372, 123310. <https://doi.org/10.1016/j.jenvman.2024.123310>.
- Chen, S., Huang, Jinliang, Huang, Jiacong, Wang, P., Sun, C., Zhang, Z., Jiang, S., 2025. Explainable deep learning identifies patterns and drivers of freshwater harmful algal blooms. *Environ. Sci. Ecotechnol.* 23, 100522. <https://doi.org/10.1016/j.esce.2024.100522>.
- Coad, P., Cathers, B., Ball, J.E., Kadluczka, R., 2014. Proactive management of estuarine algal blooms using an automated monitoring buoy coupled with an artificial neural network. *Environ. Model Softw.* 61, 393–409. <https://doi.org/10.1016/j.envsoft.2014.07.011>.
- Cruz, R.C., Reis Costa, P., Vinga, S., Krippahl, L., Lopes, M.B., 2021. A review of recent machine learning advances for forecasting harmful algal blooms and shellfish contamination. *J Mar Sci Eng* 9, 283. <https://doi.org/10.3390/jmse9030283>.
- Dai, Y., Yang, S., Zhao, D., Hu, C., Xu, W., Anderson, D.M., Li, Y., Song, X.P., Boyce, D.G., Gibson, L., Zheng, C., Feng, L., 2023. Coastal phytoplankton blooms expand and intensify in the 21st century. *Nature* 615, 280–284. <https://doi.org/10.1038/s41586-023-05760-y>.
- Davidson, K., Anderson, D.M., Mateus, M., Reguera, B., Silke, J., Sourisseau, M., Maguire, J., 2016. Forecasting the risk of harmful algal blooms. *Harmful Algae* 53, 1–7. <https://doi.org/10.1016/j.hal.2015.11.005>.
- de Lima Mendes, R., Henrick da Silva Alves, A., de Souza Gomes, M., Luiz Lima Bertarini, P., Rodrigues do Amaral, L., 2021. Many Layer Transfer Learning Genetic Algorithm (MLTLGA): a new evolutionary transfer learning approach applied to pneumonia classification. In: 2021 IEEE Congress on Evolutionary Computation (CEC). IEEE, pp. 2476–2482. <https://doi.org/10.1109/CEC45853.2021.9504912>.
- Demiray, B.Z., Mermer, O., Baydaroglu, Ö., Demir, I., 2025. Predicting harmful algal blooms using explainable deep learning models: a comparative study. *Water* 17, 676. <https://doi.org/10.3390/w17050676>.
- Dodds, W.K., Bouska, W.W., Eitzmann, J.L., Pilger, T.J., Pitts, K.L., Riley, A.J., Schloesser, J.T., Thornbrugh, D.J., 2009. Eutrophication of U. S. Freshwaters: analysis of potential economic damages. *Environ. Sci. Technol.* 43, 12–19. <https://doi.org/10.1021/es801217q>.
- Dosovitskiy, A., Beyer, L., Kolesnikov, A., Weissenborn, D., Zhai, X., Unterthiner, T., Dehghani, M., Minderer, M., Heigold, G., Gelly, S., Uszkoreit, J., Houlsby, N., 2020. An Image Is Worth 16x16 Words: Transformers for Image Recognition at Scale.
- Elliott, J.A., 2012. Is the future blue-green? A review of the current model predictions of how climate change could affect pelagic freshwater cyanobacteria. *Water research* 46 (5), 1364–1371.
- Feng, L., Yang, Y., Tan, M., Zeng, T., Tang, H., Li, Z., Niu, Z., Feng, F., 2024. Adaptive multi-source domain collaborative fine-tuning for transfer learning. *PeerJ Comput. Sci.* 10, e2107. <https://doi.org/10.7717/peerj.cs.2107>.
- Fournier, C., Fernandez-Fernandez, R., Cirés, S., López-Orozco, J.A., Besada-Portas, E., Quesada, A., 2024. LSTM networks provide efficient cyanobacterial blooms forecasting even with incomplete spatio-temporal data. *Water Res.* 267, 122553. <https://doi.org/10.1016/j.watres.2024.122553>.
- Ghafoorian, M., Mehrtash, A., Kapur, T., Karssemeijer, N., Marchiori, E., Pesteie, M., Guttmann, C.R.G., de Leeuw, F.-E., Tempany, C.M., van Ginneken, B., Fedorov, A., Abolmaesumi, P., Platel, B., Wells, W.M., 2017. Transfer Learning for Domain Adaptation in MRI: Application in Brain Lesion Segmentation. https://doi.org/10.1007/978-3-319-66179-7_59.
- Goodfellow, I., Bengio, Y., Courville, A., 2016. Deep Learning. MIT Press, Cambridge, MA.
- He, K., Girshick, R., Dollár, P., 2019. Rethinking imagenet pre-training. In: Proceedings of the IEEE/CVF International Conference on Computer Vision, pp. 4918–4927. <https://doi.org/10.1109/ICCV.2019.00502>.
- Hill, P.R., Kumar, A., Temimi, M.B.D.R., 2020. HABNet: machine learning, remote sensing-based detection of harmful algal blooms. *IEEE J Sel. Top. Appl. Earth Obs. Remote Sens.* 13, 3229–3239. <https://doi.org/10.1109/JSTARS.2020.2992902>.
- Hua, A., Gu, J., Xue, Z., Carlini, N., Wong, E., Qin, Y., 2023. Initialization Matters for Adversarial Transfer Learning 24831–24840. <https://doi.org/10.1109/CVPR52733.2024.02345>.
- Jang, Y., Lee, H., Hwang, S.J., Shin, J., 2019. Learning what and where to transfer. In: 36th Int. Conf. Mach. Learn. ICML 2019–2019–June, pp. 5360–5369.
- Janssen, A.B., Janse, J.H., Beusen, A.H., Chang, M., Harrison, J.A., Huttunen, I., Kong, X., Rost, J., Teurlincx, S., Troost, T.A., van Wijk, D., Mooij, W.M., 2019. How to model algal blooms in any lake on earth. *Curr. Opin. Environ. Sustain.* 36, 1–10. <https://doi.org/10.1016/j.cosust.2018.09.001>.
- Jia, Q., Xu, C., Jia, H., Velazquez, C., Leng, L., Yin, D., 2024. Mining spatiotemporal information for harmful algal bloom forecasting and mechanism interpreting. *ACS ES&T Water* 4 (6), 2608–2618. <https://doi.org/10.1021/acs.estwater.4c00115>.
- Kim, T., Shin, J., Lee, D., Kim, Y., Na, E., Park, J.H., Cha, Y., 2022. Simultaneous feature engineering and interpretation: forecasting harmful algal blooms using a deep learning approach. *Water Res.* 215, 118289. <https://doi.org/10.1016/j.watres.2022.118289>.
- Kim, S., Chung, S., Park, H., Cho, Y., Lee, H., 2019. Analysis of environmental factors associated with cyanobacterial dominance after river weir installation. *Water* 11 (6), 1163. <https://doi.org/10.3390/w11061163>.
- Kim, T., Shin, J., Cha, Y., 2023. Incorporation of feature engineering and attention mechanisms into deep learning models to develop an early warning system for harmful algal blooms. *J Cleaner Prod.* 414, 137564. <https://doi.org/10.1016/j.jclepro.2023.137564>.
- Kim, N., Shin, J., Cha, Y., 2024. Multisite algal bloom predictions in a lake using graph attention networks. *Environ. Eng. Res.* 29 (2). <https://doi.org/10.4491/eer.2023.210>.
- Kornblith, S., Shlens, J., Le, Q.V., 2019. Kornblith_Do_Better_ImageNet_Models_Transfer_Better_CVPR_2019_paper. Proc. IEEE Comput. Soc. Conf. Comput. Vis. Pattern Recognit. 2661–2671.
- Lee, S., Lee, D., 2018. Improved prediction of harmful algal blooms in four major South Korea's rivers using deep learning models. *Int. J. Environ. Res. Public Health* 15, 15. <https://doi.org/10.3390/ijerph15071322>.
- Li, L., Liang, Z., Liu, T., Lu, C., Yu, Q., Qiao, Y., 2025. Transformer-driven algal target detection in real water samples: from dataset construction and augmentation to model optimization. *Water (Switzerland)* 17. <https://doi.org/10.3390/w17030430>.
- Lim, B., Arik, S.O., Loeff, N., Pfister, T., 2019. Temporal Fusion Transformers for Interpretable Multi-Horizon Time Series Forecasting. <https://doi.org/10.48550/arXiv.1912.0936>.
- Lin, S., Pierson, D.C., Mesman, J.P., 2023. Prediction of algal blooms via data-driven machine learning models: an evaluation using data from a well-monitored mesotrophic lake. *Geosci. Model Dev.* 16, 35–46. <https://doi.org/10.5194/gmd-16-35-2023>.
- Lundberg, S.M., Lee, S.I., 2017. A unified approach to interpreting model predictions. *Adv. Neural Inf. Proces. Syst.* 30. <https://doi.org/10.48550/arXiv.1705.07874>.
- Ma, Y., Chen, S., Ermon, S., Lobell, D.B., 2024. Transfer learning in environmental remote sensing. *Remote Sens. Environ.* 301, 113924. <https://doi.org/10.1016/j.rse.2023.113924>.
- Marcé, R., George, G., Buscarinu, P., Deidda, M., Dunalska, J., de Eyto, E., Flaim, G., Grossart, H.-P., Istvanovics, V., Lenhardt, M., Moreno-Ostos, E., Obrador, B., Ostrovsky, I., Pierson, D.C., Potuzák, J., Poikane, S., Rinke, K., Rodríguez-Mozaz, S., Staehr, P.A., Šumberová, K., Waajen, G., Weyhenmeyer, G.A., Weathers, K.C., Zion, M., Ibelings, B.W., Jennings, E., 2016. Automatic high frequency monitoring for improved Lake and reservoir management. *Environ. Sci. Technol.* 50, 10780–10794. <https://doi.org/10.1021/acs.est.6b01604>.
- Meng, H., Zhang, J., Chang, Y., Zheng, Z., 2025. A new method for predicting chlorophyll-a concentration in a reservoir: coupling EFDC hydrodynamic and water quality model with ConvLSTM-MLP network. *J. Hydrol.* 133485. <https://doi.org/10.1016/j.jhydrol.2025.133485>.
- Mosbach, M., Andriushchenko, M., Klakow, D., 2020. On the Stability of Fine-Tuning Bert: Misconceptions, Explanations, and Strong Baselines. preprint arXiv: 2006.04884. <https://doi.org/10.48550/arXiv.2006.04884>.
- Nagae, S., Kanda, D., Kawai, S., Nobuhara, H., 2022. Automatic layer selection for transfer learning and quantitative evaluation of layer effectiveness. *Neurocomputing* 469, 151–162. <https://doi.org/10.1016/j.neucom.2021.10.051>.
- Ni, J., Liu, R., Li, Y., Tang, G., Shi, P., 2022. An improved transfer learning model for cyanobacterial bloom concentration prediction. *Water (Switzerland)* 14, 1–16. <https://doi.org/10.3390/w14081300>.
- NIER, 2023. Water Environment Information System [WWW Document].
- Paerl, H.W., Huisman, J., 2008. Blooms like it hot. *Science* 320, 57–58. <https://doi.org/10.1126/science.1155398>.
- Paerl, H.W., Otten, T.G., 2013. Harmful cyanobacterial blooms: causes, consequences, and controls. *Microb. Ecol.* 65, 995–1010. <https://doi.org/10.1007/s00248-012-0159-y>.
- Park, H.K., Lee, H.J., Heo, J., Yun, J.H., Kim, Y.J., Kim, H.M., Lee, I.J., 2021. Deciphering the key factors determining spatio-temporal heterogeneity of cyanobacterial bloom dynamics in the Nakdong River with consecutive large weirs. *Sci. Total Environ.* 755, 143079. <https://doi.org/10.1016/j.scitotenv.2020.143079>.
- Peng, L., Wu, H., Gao, M., Yi, H., Xiong, Q., Yang, L., Cheng, S., 2022. TLT: recurrent fine-tuning transfer learning for water quality long-term prediction. *Water Res.* 225, 119171. <https://doi.org/10.1016/j.watres.2022.119171>.

- Rousoo, B.Z., Bertone, E., Stewart, R., Hamilton, D.P., 2020. A systematic literature review of forecasting and predictive models for cyanobacteria blooms in freshwater lakes. *Water Res.* 182, 115959. <https://doi.org/10.1016/j.watres.2020.115959>.
- Schmidhuber, J., 2015. Deep learning. *Scholarpedia* 10, 32832. <https://doi.org/10.4249/scholarpedia.32832>.
- Shin, J., Cha, Y., 2025. Development of a deep learning-based feature stream network for forecasting riverine harmful algal blooms from a network perspective. *Water Res.* 268, 122751. <https://doi.org/10.1016/j.watres.2024.122751>.
- Shin, Y., Kim, T., Hong, S., Lee, S., Lee, E., Hong, S.W., Lee, C.S., Kim, T.Y., Park, M.S., Park, J., Heo, T.Y., 2020. Prediction of chlorophyll-a concentrations in the Nakdong river using machine learning methods. *Water (Switzerland)* 12. <https://doi.org/10.3390/w12061822>.
- Shin, J., Yoon, S., Cha, Y., 2017. Prediction of cyanobacteria blooms in the lower Han River (South Korea) using ensemble learning algorithms. *Desalination and Water Treatment* 84, 31–39. <https://doi.org/10.5004/dwt.2017.20986>.
- Subel, A., Guan, Y., Chattopadhyay, A., Hassanzadeh, P., 2023. Explaining the physics of transfer learning in data-driven turbulence modeling. *PNAS Nexus* 2, 1–14. <https://doi.org/10.1093/pnasnexus/pgad015>.
- Vaswani, A., Shazeer, N., Parmar, N., Uszkoreit, J., Jones, L., Gomez, A.N., Kaiser, L., Polosukhin, I., 2017. Attention Is all you Need.
- Vrbancic, G., Podgorelec, V., 2020. Transfer learning with adaptive fine-tuning. *IEEE Access* 8, 196197–196211. <https://doi.org/10.1109/ACCESS.2020.3034343>.
- Wang, S., Gao, M., Wu, H., Luo, F., Jiang, F., Tao, L., 2024. Many-to-many: domain adaptation for water quality prediction. *Appl. Soft Comput.* 167, 112381. <https://doi.org/10.1016/j.asoc.2024.112381>.
- Weiss, K., Khoshgoftaar, T.M., Wang, D.D., 2016. A Survey of Transfer Learning. *Journal of Big Data*. Springer International Publishing. <https://doi.org/10.1186/s40537-016-0043-6>.
- Wells, M.J., Trainer, V.L., Smayda, T.J., Karlson, B.S.O., Trick, C.G., Kudela, R.M., Ishikawa, A., Bernard, S., Wulff, A., Anderson, D.M., Cochlan, W.P., 2015. Past and present to forecast the future. *Harmful Algae* 1, 68–93. <https://doi.org/10.1016/j.hal.2015.07.009.Harmful>.
- Xu, J., Fan, H., Luo, M., Li, P., Jeong, T., Xu, L., 2023. Transformer based water level prediction in Poyang Lake. *China. Water (Switzerland)* 15. <https://doi.org/10.3390/w15030576>.
- Yussof, F.N., Maan, N., Reba, M.N.M., 2021. LSTM networks to improve the prediction of harmful algal blooms in the west coast of Sabah. *Int. J. Environ. Res. Public Health* 18. <https://doi.org/10.3390/ijerph18147650>.
- Zhu, X., Wu, X., 2004. Class noise vs. attribute noise: a quantitative study. *Artif. Intell. Rev.* 22, 177–210. <https://doi.org/10.1007/s10462-004-0751-8>.
- Zhu, N., Ji, X., Tan, J., Jiang, Y., Guo, Y., 2021. Prediction of dissolved oxygen concentration in aquatic systems based on transfer learning. *Comput. Electron. Agric.* 180, 105888. <https://doi.org/10.1016/j.compag.2020.105888>.
- Zhuang, F., Qi, Z., Duan, K., Xi, D., Zhu, Y., Zhu, H., Xiong, H., He, Q., 2021. A comprehensive survey on transfer learning. *Proc. IEEE* 109, 43–76. <https://doi.org/10.1109/JPROC.2020.3004555>.
- Zunair, H., Mohammed, N., Momen, S., 2018. Unconventional wisdom: a new transfer learning approach applied to Bengali numeral classification. In: 2018 Int. Conf. Bangla Speech Lang. Process. ICBSLP, 2018, pp. 1–6. <https://doi.org/10.1109/ICBSLP.2018.8554435>.